Hidden Quasiparticles and Incoherent Photoemission Spectra in Na_2IrO_3

Fabien Trousselet,[1,2] Mona Berciu,[3,4] Andrzej M. Oleś,[1,5] and Peter Horsch[1]

[1]*Max-Planck-Institut für Festkörperforschung, Heisenbergstrasse 1, D-70569 Stuttgart, Germany*
[2]*Institute Néel, CNRS/UJF, 25 Avenue des Martyrs, BP166, F-38042 Grenoble Cedex 9, France*
[3]*Department of Physics and Astronomy, University of British Columbia, Vancouver, British Columbia, Canada V6T 1Z1*
[4]*Quantum Matter Institute, University of British Columbia, Vancouver, British Columbia, Canada V6T 1Z4*
[5]*Marian Smoluchowski Institute of Physics, Jagellonian University, Reymonta 4, PL-30059 Kraków, Poland*

(Received 1 February 2013; published 19 July 2013)

We study two Kitaev-Heisenberg t-J-like models on a honeycomb lattice, focusing on the zigzag magnetic phase of Na_2IrO_3, and investigate hole motion by exact diagonalization and variational methods. The spectral functions are quite distinct from those of cuprates and are dominated by large incoherent spectral weight at high energy, almost independent of the microscopic parameters—a universal and generic feature for zigzag magnetic correlations. We explain why quasiparticles at low energy are strongly suppressed in the photoemission spectra and determine an analog of a pseudogap. We point out that the qualitative features of the predominantly incoherent spectra obtained within the two different models for the zigzag phase are similar, and they have a remarkable similarity to recently reported angular resolved photoemission spectra for Na_2IrO_3.

DOI: 10.1103/PhysRevLett.111.037205 PACS numbers: 75.10.Jm, 72.10.Di, 75.25.Dk, 79.60.−i

Frustrated spin systems have long served as a rich source of exotic phenomena such as unconventional magnetic order or spin liquid behavior [1,2]. A beautiful realization of a spin liquid is found in the Kitaev model [3], where bond-dependent Ising interactions lead to strong frustration on the two-dimensional (2D) honeycomb lattice. While antiferromagnetic (AF) or ferromagnetic (FM) couplings are equivalent, a FM realization was originally suggested [4]. The Kitaev model is exactly solvable and has spin correlations that vanish beyond nearest neighbor (NN) spins [5]. This spin liquid is robust against weak time-reversal invariant perturbations, including the Heisenberg ones [6,7], similar to the spin-orbital liquid in the SU(4) symmetric Kugel-Khomskii model [8], but in striking contrast to the 2D compass model [9].

Such peculiar, highly anisotropic interactions are believed to be realized in A_2IrO_3 (A = Na, Li) iridates where strong spin-orbit coupling generates Kramers doublets of isospin states [4,10]. These systems are Mott insulators as confirmed by the electronic structure [11,12]. It has been suggested [4,6] that effective $S = 1/2$ pseudospins, standing for locally spin-orbital-entangled t_{2g} states [13,14], interact via competing AF Heisenberg and FM Kitaev exchange couplings between NNs in the Kitaev-Heisenberg (KH) model—this scenario is consistent with the magnetic susceptibility [15] and with resonant inelastic x-ray scattering [16]. Surprisingly, the theoretical predictions of a spin liquid or stripy AF phase [6] were not confirmed but instead zigzag AF order, consisting of staggered FM zigzag chains, was found in Na_2IrO_3 [17–20]. To stabilize this phase next-nearest neighbor (NNN) and third nearest neighbor (3NN) AF Heisenberg terms [21] have been invoked in the KH model [22]. Recently a simpler scenario, including e_g orbitals in the exchange paths [23], has been proposed [24]; there, the zigzag AF phase emerges in a broad range of parameters in the KH model when the signs of all NN exchange terms are *inverted*.

In this Letter we investigate whether hole motion in an effective KH model can explain recent angle-resolved photoemission spectroscopy (ARPES) experiments for Na_2IrO_3 [11]. One expects that a hole might move coherently along the FM zigzag chain [Fig. 1(a)], similar to free hole propagation in states with ferro-order of t_{2g} orbitals [25]. It is therefore quite surprising that the ARPES spectra for Na_2IrO_3 are dominated instead by incoherent spectral weight found predominantly at high energy [11]. This poses several intriguing questions: (i) Can we make use

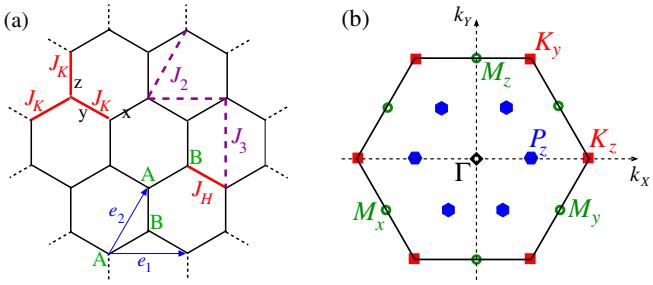

FIG. 1 (color online). Honeycomb lattice of Ir ions in Na_2IrO_3: (a) cluster of $N = 24$ sites, and the elementary translations $\vec{e}_{1(2)}$ within two sublattices A or B (for two NN A atoms $a = 1$). Exchange couplings are in Heisenberg (J_H) and Kitaev (J_K) (solid line); Heisenberg NNN (J_2) and 3NN (J_3) (dashed line). (b) First Brillouin zone with high symmetry points: Γ, $M_y = (\pi, -\pi/\sqrt{3})$, $K_z = (4\pi/3, 0)$; in exact diagonalization M_γ and K_γ are equivalent ($\gamma \in \{x, y, z\}$) and called M and K.

of ARPES results to identify the relevant scenario for zigzag ordering? (ii) Is there any similarity between the present ARPES results and those known for cuprates [26], described by quasiparticles (QPs) within the t-J model [27,28]? (iii) Are the spectra determined by entangled spin-orbital excitations [29], or by composite fermions emerging from spin-orbit interaction [4]? (iv) Is the incoherent hole scattering on spin excitations as important here as between the FM planes of $LaMnO_3$ [30]? We answer these questions below and show that weak QPs exist but are hidden for the present honeycomb lattice so that ARPES reveals the incoherent processes.

We consider the following t-J-like model ($t > 0$),

$$\mathcal{H}_{tJ} \equiv \mathcal{H}_t + \mathcal{H}_J = t\sum_{\langle ij\rangle\sigma} c^\dagger_{i\sigma}c_{j\sigma} + J_H\sum_{\langle ij\rangle}\vec{S}_i\cdot\vec{S}_j + J_K\sum_{\langle ij\rangle_\gamma} S^\gamma_i S^\gamma_j, \quad (1)$$

on the honeycomb lattice [Fig. 1(a)], called *model I*. The hopping $\mathcal{H}_t$ of composite fermions with pseudospin flavor σ [31] (contributions from direct d-d and d-p-d hopping [32]) occurs in the restricted space without double occupancies due to large on-site Coulomb repulsion U, and the exchange $\mathcal{H}_J$ stands for the KH model—with FM Heisenberg ($J_H < 0$) and AF Kitaev ($J_K > 0$) exchange,

$$J_H \equiv -J(1-\alpha), \qquad J_K \equiv 2J\alpha. \quad (2)$$

Here J is the energy unit and $\alpha \in [0, 1]$ interpolates between the Heisenberg and Kitaev exchange couplings for NN 1/2 spins $\{\vec{S}_i\}$; the zigzag AF phase (Fig. 2) is found in a broad range of α [24]. We also investigate the spectral functions in *model II*, where exchange couplings $-\mathcal{H}_J$ are extended by NNN and 3NN terms $J_n = J(1-\alpha)j_n > 0$:

$$\mathcal{H}'_{tJ} = \mathcal{H}_t - \mathcal{H}_J + \Big\{J_2\sum_{\{ij\}\in\mathrm{NNN}}\vec{S}_i\cdot\vec{S}_j + J_3\sum_{\{ij\}\in 3\mathrm{NN}}\vec{S}_i\cdot\vec{S}_j\Big\}. \quad (3)$$

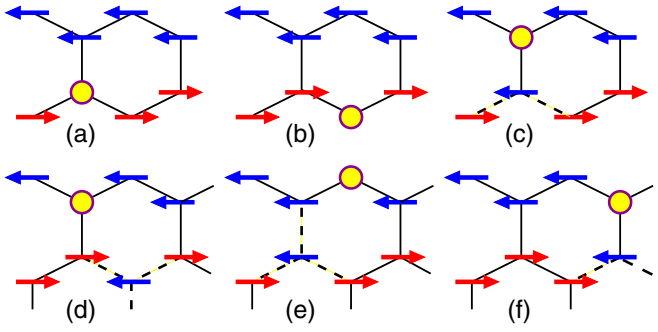

FIG. 2 (color online). Artist's view of hole propagation in the zigzag phase of Na_2IrO_3 (arrows). (a) The hole (circle) may either (b) propagate along the FM chain by *intrachain* hopping t, or (c) create a magnon by *interchain* hopping $t_\perp$. Either this spin defect (d) or the hole (e) can move along its chain. (f) After two steps (d) + (e) the hole and the defect may recombine. Broken bonds are indicated by dashed lines.

Although our aim is to present the spectral functions obtained by exact diagonalization (ED) for a hole in the quantum-fluctuating zigzag AF phase, we begin with describing the physical processes and resulting spectral properties of a hole inserted into a fully polarized zigzag ground state $|0\rangle$; see Fig. 2(a). The hole hopping is isotropic, but for convenience we distinguish *intrachain* hopping t and *interchain* hopping $t_\perp$. Free hole propagation, see Fig. 2(b), occurs along the 1D FM zigzag chain when $t_\perp = 0$. It involves two types of Ir sites that belong to sublattices A and B; see Fig. 1(a). We are interested in the spectral properties measured in the ARPES experiment with the hole creation operator $c^\dagger_{\vec{k}\uparrow}$, and we also consider the hole creation on sublattice A, $d^\dagger_{\vec{k}\uparrow}$ [33]:

$$d^\dagger_{\vec{k}\uparrow} \equiv \sqrt{\frac{2}{N}}\sum_{i\in A} e^{i\vec{k}\cdot\vec{r}_i}c^\dagger_{i\uparrow}, \qquad c^\dagger_{\vec{k}\uparrow} \equiv \frac{1}{\sqrt{N}}\sum_i e^{i\vec{k}\cdot\vec{r}_i}c^\dagger_{i\uparrow}. \quad (4)$$

As we shall see, the sublattice aspect is rather subtle and responsible for the hidden QP states in the ARPES experiments for the zigzag phase. The spectral functions

$$A_f(\vec{k},\omega) = \frac{1}{\pi}\Im\langle 0|f^\dagger_{\vec{k}\uparrow}\frac{1}{\omega - i\eta + E_0 - \mathcal{H}}f_{\vec{k}\uparrow}|0\rangle, \quad (5)$$

correspond to the physical Green's function $G_c(\vec{k},\omega)$ for $f \equiv c$, or to the sublattice Green's function $G_d(\vec{k},\omega)$ for $f \equiv d$ (4); here E_0 is the energy of the ground state $|0\rangle$.

Below we describe and use a variational approach well adapted to the perturbative regime ($|t| \ll J$) to gain more physical insights. We write the KH t-J model (1) as $\mathcal{H}_{tJ} \equiv \mathcal{H}_0 + \mathcal{V}$, with an exactly solvable part $\mathcal{H}_0$ and the perturbation $\mathcal{V}$. When exchange interactions are Ising-like, either in spin [34] or in orbital [25] systems, the number of magnons (orbitons) is conserved and the classical ground state $|0\rangle$ is exact. Here we use the same strategy to develop a variational treatment [35] and include in $\mathcal{H}_0$ all terms that conserve the number of magnons, while $\mathcal{V}$ includes the interchain hole hopping that creates or removes a spin excitation [Fig. 2(c)] together with exchange terms generating magnon pairs.

When a hole moves to a neighboring chain, it creates a spin defect with energy $\varepsilon^{(0)}_m = |J_H|$; see Fig. 2(c). The defect propagates as a magnon [Fig. 2(d)], and the hole can also move by hopping t [Fig. 2(e)] along the FM chain. Both processes generate two parallel spins on a vertical (interchain) bond and increase the magnon energy to $\varepsilon_m = |J_H| + (J_K + J_H)/2$, but a hole and a spin defect may also meet at one vertical bond [Fig. 2(f)], which decreases the magnon energy back to $\varepsilon^{(0)}_m$. All these processes cause incoherence. Other states with several spin defects cost too much energy when $J \gg t$—these states are neglected in the one-magnon variational treatment.

In the zigzag phase we write Dyson's equation, $G(\omega) = G^0(\omega) + G(\omega)\mathcal{V}G^0(\omega)$, for the resolvent, $G(\omega) \equiv \{\omega - i\eta + E_0 - \mathcal{H}\}^{-1}$. The Green's functions

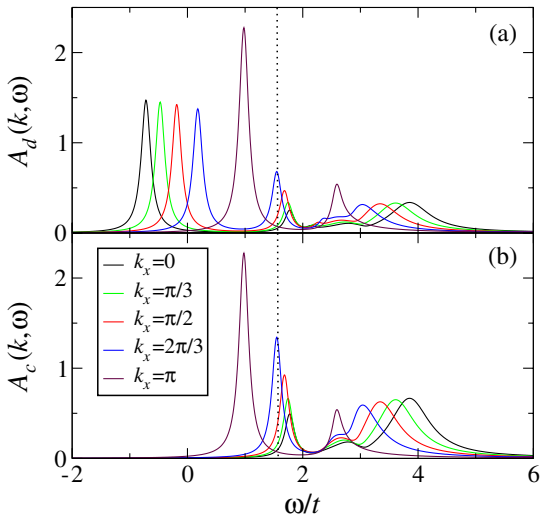

FIG. 3 (color online). Spectral functions as obtained for model I (1) in the one-magnon approximation: (a) $A_d(k_x, \omega)$ and (b) $A_c(k_x, \omega)$ (5). The dashed line indicates the static hole energy ϵ_0. Parameters: $\alpha = 5/9$, $t/J = 0.25$, and $\eta = 0.1t$.

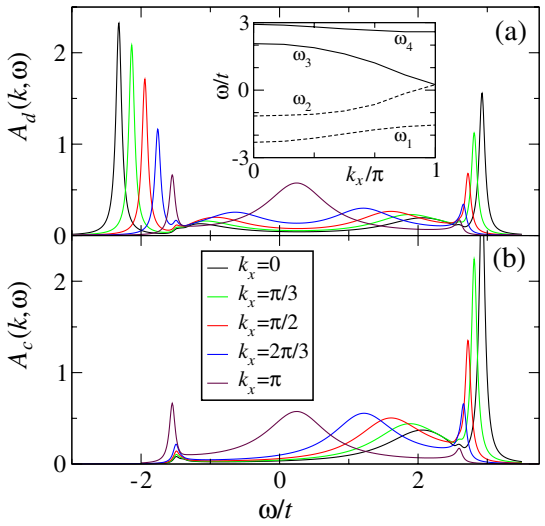

FIG. 4 (color online). Spectral functions as obtained for model I (1) in the one-magnon approximation: (a) $A_d(k_x, \omega)$ and (b) $A_c(k_x, \omega)$ (5). The inset shows k_x dependence of the frequencies ω_i corresponding to the four distinct features visible in $A_d(k_x, \omega)$; the ω_1 and ω_2 ones are hidden in $A_c(k_x, \omega)$. Parameters: $\alpha = 5/9$, $t/J = 2.0$ and $\eta = 0.1t$.

$G_d(\vec{k}, \omega)$ obtained from it are 2×2 matrices for two sublattices, A and B. The unperturbed Green's function, $G_d^0(\vec{k}, \omega)$, is found exactly—it describes free propagation of a hole along the FM chains, and depends on 1D momentum k_x [Fig. 1(b)], $\varepsilon_{\vec{k}\pm} = \epsilon_0 \mp 2t\cos(k_x/2)$, with $\epsilon_0 = 1/4J(1+\alpha)$ being the energy of a static hole. The two $\pm$ states for each k_x result from band folding associated with the two-site unit cell, independent of the 1D nature of hole motion. These states give two QPs at each momentum k_x in $A_d^{(0)}(k_x, \omega)$, except at $k_x = \pi$ where $\varepsilon_{\vec{k}\pm} = \epsilon_0$. In contrast, in $A_c^{(0)}(k_x, \omega)$, the lower energy QP, $\varepsilon_{\vec{k}+}$, is *hidden*, while the higher energy one, $\varepsilon_{\vec{k}-}$, has twice larger spectral weight, due to interference between the two sublattice contributions.

The difference between $A_d(\vec{k}, \omega)$ and $A_c(\vec{k}, \omega)$ (5) for model I, that follows from the states' parity, is well visible in the weak coupling regime of $J \gg t$; see Fig. 3 [36]. At low energy, $\omega < \epsilon_0$, one finds QPs in $A_d(k_x, \omega)$ but not in $A_c(k_x, \omega)$. The width of the QP band is somewhat reduced from the expected $2t$, but even stronger renormalization (its width is lower than t) is found for $\omega > \epsilon_0$. New incoherent features observed in both spectral functions (5) above $\omega = 2t$ (Fig. 3) are generated by a magnon excitation due to the interchain hopping $t_\perp$; see Fig. 2(c). These states disperse on the scale of $\sim 2t$ (with energy difference between the respective maxima at $k_x = 0$ and π being $\simeq 1.4t$) and we recognize here the propagation of a *holon* [37,38].

In the intermediate coupling regime $t > J$, the spectral weight moves to higher energies (Fig. 4). First, one recognizes distinct QPs in $A_d(\vec{k}, \omega)$ [*hidden* in $A_c(\vec{k}, \omega)$], with further decreased total width of this subband and the spectral weight decreasing from $k_x = 0$ to π. This follows from hole scattering on magnon excitations (Fig. 2) that become gradually more important when t/J increases. Second, the spectra $A_c(\vec{k}, \omega)$ at $t/J = 2.0$ [Fig. 4(b)] have three notable features: (i) the suppressed QP peaks at the onset of the spectrum at low energy, (ii) the upper holon branch, with spectral weight moving to higher energies when k_x decreases from π to 0, and (iii) large spectral weight with weak momentum dependence at the upper edge of the spectrum. These higher energy features are expected to be strongly renormalized when the constraint to one-magnon excitations is lifted. In contrast, the QPs disappear in the strong coupling regime $t \gg J$ as well, because the destructive interference is due to parity.

Indeed, the unbiased ED [39] performed on a periodic cluster of $N = 24$ sites [Fig. 1(a)] for model I with the same $\alpha = 5/9$ yields very incoherent spectral weight distribution in $A_c(\vec{k}, \omega)$, see Fig. 5(a), in contrast to the 2D t-J model [28,40]. The most important feature is that the spectral weight is moved to high energy for the P and Γ points. At the M point one observes a broad feature at $\omega/t \simeq 0.3$, accompanied by a shoulder at $\omega \simeq 2.5t$, and a small QP peak at $\omega \simeq -2.5t$—such a peak is also observed at K but absent for momenta inside the Brillouin zone (BZ). The spectral weight is transferred from high to lower energy when one moves from the Γ point to the edge of the BZ (M and K points). These qualitative features are generic and hold in a broad range of parameters, but weak QPs emerge for increasing Kitaev coupling (see Supplemental Material [41]).

The spectral weight is distributed quite differently in $A_d(\vec{k}, \omega)$ [Fig. 5(b)]. Here QP peaks appear for all momenta

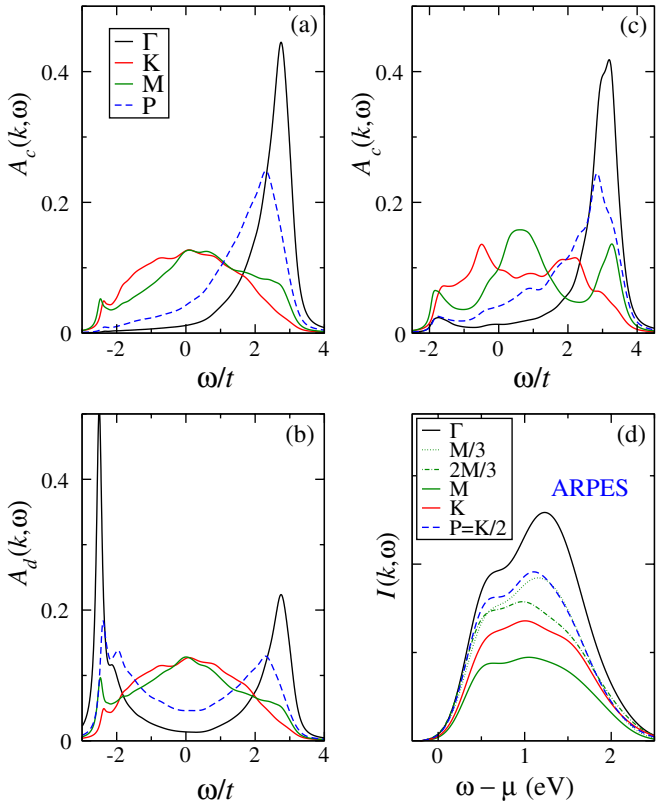

FIG. 5 (color online). Spectral functions as obtained by ED for $N = 24$ sites at selected high-symmetry points Γ, K, M, and P in the BZ at $t/J = 5$ and $\eta = 0.1t$: (a) $A_c(\vec{k}, \omega)$ and (b) $A_d(\vec{k}, \omega)$, both for model I (1) with $\alpha = 5/9$; (c) $A_c(\vec{k}, \omega)$ for model II (3), with $\alpha = 0.4$, $j_2 = 0.2$, and $j_3 = 0.5$. ARPES spectra for Na_2IrO_3 [11] with background subtracted [43] are shown in (d) for the selected $\vec{k}$ points [44].

at energies $\omega < -2t$, with much more weight than those observed in $A_c(\vec{k}, \omega)$, and there is strong spectral weight transfer to low energies at P and Γ points. The QP weight is maximal for Γ and small for K or M point, as expected from the variational approach [Fig. 4(a)]. We suggest that the lowest energy QP at the Γ point determines the chemical potential μ and is responsible for the experimentally seen *pseudogap* of $\Delta \sim 0.35$ eV [11].

It is quite remarkable that the ED results obtained with model II [Fig. 5(c)] for parameters suggested [19] for Na_2IrO_3, are qualitatively similar to those found in model I [Fig. 5(a)] but have a somewhat richer structure. At the M point one finds a two-peak structure with a weak QP at the low energy side, which develops to a shoulder at the K point. The spectra found at P and Γ points look similar to those of model I, again with most of the weight concentrated at high energy. The broad incoherent spectral weight and its shift to higher energy between the K and Γ point are recognized here as universal features for the parameters favoring the zigzag phase. Indeed, moderate changes of parameters (α, and in addition j_2, j_3 for model II) modifying the degree of frustration while still supporting the zigzag order, do not lead to emerging QPs (see Supplemental Material [41]).

We suggest that the ED [39] simulates here the main features of the ARPES spectra measured at $T = 130$ K [11]—although the Néel temperature $T_N \simeq 15$ K is much smaller due to frustration, the incoherent part of the spectra should be only weakly affected by thermal fluctuations for $T \lesssim J$. Indeed, zigzag-type spin-spin correlations subsist at $T \simeq 130$ K (see Supplemental Material [41]). The spectra are incoherent and no QPs are seen at the low edge $\omega \simeq \mu$, see Fig. 5(d). With the total width of the spectrum $\sim 6t$ we estimate that $t \simeq 0.3$ eV. Large spectral weight at the Γ and P points is seen mostly at high energy, as in the ED in $A_c(\vec{k}, \omega)$ but not in $A_d(\vec{k}, \omega)$ [Figs. 5(a) and 5(b)]. At K and M one recognizes three characteristic features with appreciable spectral weight in the ARPES data [11] at $\omega - \mu \simeq 0.6$ [42], $\simeq 1.1$, and $\simeq 1.5$ eV that have some correspondence in the ED spectra. The basic features of the ARPES spectra, (i) the strong incoherence and (ii) the shift of the spectral weight to high energies at the P and Γ points, are dictated by the zigzag correlations and are similar in the two models. Yet, we notice differences in the fine structure that reflect the dramatically different underlying Hamiltonians, and therefore suggest that model I is closer to the experimental data [11].

Summarizing, we have shown that essential features seen in recent ARPES experiments for Na_2IrO_3 [11] may be described by a universal phenomenology that does not depend on details of modeling. The framework used is a t-J-like model with nearest neighbor Kitaev and Heisenberg exchange, having conceptually some similarity to high T_c cuprates. The physical spectral function $A_c(\vec{k}, \omega)$ in the strong coupling regime explains qualitatively the incoherent nature of the ARPES spectra, with large spectral weight at high energy and the pseudogap determined by hidden quasiparticles at low energy. This also confirms that the low-energy electronic structure of Na_2IrO_3 can be described by the motion of composite $j = 1/2$ fermions due to strong spin-orbit coupling.

As a challenge to future ARPES experiments, we suggest that the spectra of Li_2IrO_3, with stronger Kitaev coupling than in Na_2IrO_3 [24], would be incoherent but could also show weak quasiparticles. A more quantitative analysis is beyond the scope of the present study as it would require additional information concerning matrix elements in the ARPES experiment.

We thank Andrea Damascelli, Lou-Fe' Feiner, George Jackeli, Giniyat Khaliullin, George A. Sawatzky, and Ignacio Hamad for insightful discussions. We are grateful to Riccardo Comin for providing the experimental data of Ref. [11]. This work was supported by the Max Planck–UBC Centre for Quantum Materials; F. T. thanks Advanced Materials and Process Engineering Laboratory (AMPEL),

University of British Columbia, Vancouver, for kind hospitality. A. M. O. kindly acknowledges support by the Polish National Science Center (NCN) under Project No. 2012/04/A/ST3/00331.

[1] Leon Balents, Nature (London) **464**, 199 (2010).
[2] B. Normand, Contemp. Phys. **50**, 533 (2009).
[3] A. Kitaev, Ann. Phys. (Amsterdam) **321**, 2 (2006).
[4] G. Jackeli and G. Khaliullin, Phys. Rev. Lett. **102**, 017205 (2009).
[5] G. Baskaran, S. Mandal, and R. Shankar, Phys. Rev. Lett. **98**, 247201 (2007).
[6] J. Chaloupka, G. Jackeli, and G. Khaliullin, Phys. Rev. Lett. **105**, 027204 (2010).
[7] J. Reuther, R. Thomale, and S. Trebst, Phys. Rev. B **84**, 100406 (2011); R. Schaffer, S. Bhattacharjee, and Y. B. Kim, *ibid.* **86**, 224417 (2012).
[8] P. Corboz, M. Lajkó, A. M. Läuchli, K. Penc, and F. Mila, Phys. Rev. X **2**, 041013 (2012).
[9] F. Trousselet, A. M. Oleś, and P. Horsch, Europhys. Lett. **91**, 40 005 (2010); Phys. Rev. B **86**, 134412 (2012).
[10] A. Shitade, H. Katsura, J. Kuneš, X.-L. Qi, S.-C. Zhang, and N. Nagaosa, Phys. Rev. Lett. **102**, 256403 (2009).
[11] R. Comin *et al.*, Phys. Rev. Lett. **109**, 266406 (2012).
[12] Insulating state follows also from quasimolecular orbitals; see I. I. Mazin, H. O. Jeschke, K. Foyevtsova, R. Valentí, and D. I. Khomskii, Phys. Rev. Lett. **109**, 197201 (2012).
[13] P. Horsch, G. Khaliullin, and A. M. Oleś, Phys. Rev. Lett. **91**, 257203 (2003).
[14] A. M. Oleś, J. Phys. Condens. Matter **24**, 313201 (2012).
[15] Y. Singh and P. Gegenwart, Phys. Rev. B **82**, 064412 (2010); F. Trousselet, G. Khaliullin, and P. Horsch, *ibid.* **84**, 054409 (2011).
[16] H. Gretarsson *et al.*, Phys. Rev. Lett. **110**, 076402 (2013).
[17] X. Liu, T. Berlijn, W.-G. Yin, W. Ku, A. Tsvelik, Y.-J. Kim, H. Gretarsson, Y. Singh, P. Gegenwart, and J. P. Hill, Phys. Rev. B **83**, 220403 (2011).
[18] Y. Singh, S. Manni, J. Reuther, T. Berlijn, R. Thomale, W. Ku, S. Trebst, and P. Gegenwart, Phys. Rev. Lett. **108**, 127203 (2012).
[19] S. K. Choi *et al.*, Phys. Rev. Lett. **108**, 127204 (2012).
[20] F. Ye, S. Chi, H. Cao, B. C. Chakoumakos, J. A. Fernandez-Baca, R. Custelcean, T. F. Qi, O. B. Korneta, and G. Cao, Phys. Rev. B **85**, 180403 (2012).
[21] The zigzag phase is stable in the J_1-J_2-J_3 model on the honeycomb lattice; see A. F. Albuquerque, D. Schwandt, B. Hetényi, S. Capponi, M. Mambrini, and A. M. Läuchli, Phys. Rev. B **84**, 024406 (2011); J. Reuther, D. A. Abanin, and R. Thomale, *ibid.* **84**, 014417 (2011).
[22] I. Kimchi and Y.-Z. You, Phys. Rev. B **84**, 180407 (2011).
[23] G. Khaliullin, Prog. Theor. Phys. Suppl. **160**, 155 (2005).
[24] J. Chaloupka, G. Jackeli, and G. Khaliullin, Phys. Rev. Lett. **110**, 097204 (2013).
[25] M. Daghofer, K. Wohlfeld, A. M. Oleś, E. Arrigoni, and P. Horsch, Phys. Rev. Lett. **100**, 066403 (2008); P. Wróbel and A. M. Oleś, *ibid.* **104**, 206401 (2010).
[26] A. Damascelli, Z. Hussain, and Z.-X. Shen, Rev. Mod. Phys. **75**, 473 (2003).
[27] G. Martinez and P. Horsch, Phys. Rev. B **44**, 317 (1991); J. Bonča, S. Maekawa, and T. Tohyama, *ibid.* **76**, 035121 (2007); I. J. Hamad, A. E. Trumper, A. E. Feiguin, and L. O. Manuel, *ibid.* **77**, 014410 (2008).
[28] Elbio Dagotto, Rev. Mod. Phys. **66**, 763 (1994).
[29] K. Wohlfeld, A. M. Oleś, and P. Horsch, Phys. Rev. B **79**, 224433 (2009).
[30] J. Bała, G. A. Sawatzky, A. M. Oleś, and A. Macridin, Phys. Rev. Lett. **87**, 067204 (2001).
[31] T. Hyart, A. R. Wright, G. Khaliullin, and B. Rosenow, Phys. Rev. B **85**, 140510 (2012); Y.-Z. You, I. Kimchi, and A. Vishwanath, *ibid.* **86**, 085145 (2012).
[32] G. Khaliullin, W. Koshibae, and S. Maekawa, Phys. Rev. Lett. **93**, 176401 (2004).
[33] A. Lüscher, A. Läuchli, W. Zheng, and O. P. Sushkov, Phys. Rev. B **73**, 155118 (2006).
[34] S. A. Trugman, Phys. Rev. B **37**, 1597 (1988).
[35] M. Berciu and H. Fehske, Phys. Rev. B **84**, 165104 (2011); M. Möller, G. A. Sawatzky, and M. Berciu, *ibid.* **86**, 075128 (2012).
[36] The value $\alpha \simeq 5/9$ fits well the susceptibility data [18,24].
[37] M. Daghofer and P. Horsch, Phys. Rev. B **75**, 125116 (2007).
[38] P. Phillips, Rev. Mod. Phys. **82**, 1719 (2010).
[39] No symmetry breaking associated to a particular zigzag pattern occurs in the present ED approach.
[40] K. J. von Szczepanski, P. Horsch, W. Stephan, and M. Ziegler, Phys. Rev. B **41**, 2017 (1990); A. Ramšak and P. Horsch, *ibid.* **57**, 4308 (1998).
[41] See the Supplemental Material at http://link.aps.org/supplemental/10.1103/PhysRevLett.111.037205 for more technical details.
[42] The ED does not reproduce this low energy excitation with no $\vec{k}$ dependence that might correspond to $j = 3/2$ states, absent in the effective t-J-like model Eq. (1).
[43] The norm of $A_c(\vec{k}, \omega)$ in ED is $1/2$ at half-filling as expected for constrained fermions, see W. Stephan and P. Horsch, Phys. Rev. Lett. **66**, 2258 (1991). In contrast, $I(\vec{k}, \omega)$ obeys no sum rule because of matrix elements and background subtraction.
[44] As in our definition of $A(\vec{k}, \omega)$ Eq. (5), we plot increasing ARPES excitation energies in $I(\vec{k}, \omega)$ from left to right.